Inorganic Chemistry

Article

pubs.acs.org/IC

Heterodinuclear Metal Arrangement in a Flat Macrocycle with Two Chemically- Equivalent Metal Chelating Sites

Masumi Kuritani, Shohei Tashiro, and Mitsuhiko Shionoya*

Department of Chemistry, Graduate School of Science, The University of Tokyo, 7-3-1 Hongo, Bunkyo-ku, Tokyo 113-0033, Japan

Supporting Information

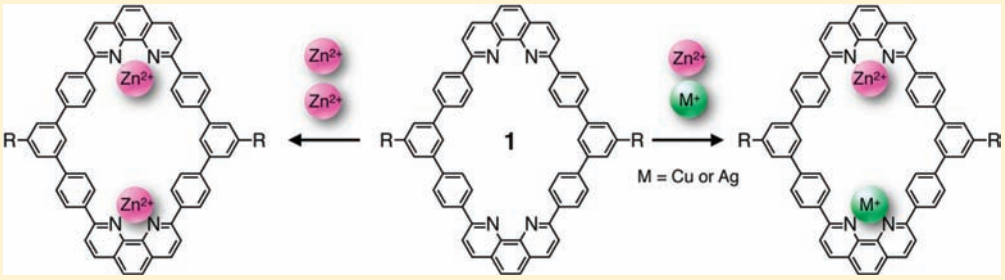

ABSTRACT: A phenanthroline-based macrocycle **1** has been newly developed which has two chemically equivalent metal chelating sites within the spatially restricted cavity for dinuclear metal arrangement. The macrocycle **1** reacts with $Zn(CF_3CO_2)_2$ or $ZnCl_2$ to form homodinuclear Zn(II)-complexes. A single-crystal X-ray structural analysis of the resulting $Zn_2\mathbf{1}(CF_3CO_2)_4$ determined the complex structure in which two Zn(II) ions are bound by two phenanthroline sites and two $CF_3CO_2^-$ ions bind to each Zn(II) ion in a tetrahedral geometry. Similarly, a homodinuclear Cu(I)-macrocycle was formed from **1** and $Cu(CH_3CN)_4BF_4$. Notably, from **1** and an equimolar mixture of $Cu(CH_3CN)_4BF_4$ and $Zn(CF_3CO_2)_2$, a heterodinuclear Cu(I)−Zn(II)-macrocycle was exclusively formed in high yield (>90%) because of the relatively low stability of the dinuclear Cu(I)-macrocycle. A heterodinuclear Ag(I)−Zn(II)-macrocycle was similarly formed with fairly high selectivity from a mixture of Ag(I) and Zn(II) ions. Such selective heterodinuclear metal arrangement was not observed with other combinations of M-Zn(II) (M = Li(I), Mg(II), Pd(II), Hg(II), La(III), and Tb(III)).

INTRODUCTION

In recent years, a number of examples of organic macrocycles capable of binding multiple metal ions within their inner space have been reported. These macrocyclic ligands possess centrally directed coordination sites such as Schiff base,[1] pyrrole,[2] pyridine ring,[3] amine,[4] phosphine,[5] sulfide,[6] and so on. Such metallo-macrocycles are known to have metal-centered chemical functions such as anion[1m,4a,5] and cation[1g,j,l] recognition, activation of reacting molecules,[3b,4d,e] metal assembly,[1d−f,h,6d] spontaneous stacking,[1i−k] or construction of distinctive topological molecules.[1n,2d,3c] The relationship between their structures and functions highly depends on the number, kind, and arrangement of metal ions. In particular, it is getting more challenging to develop heteronuclear metal arrangement within one molecule to give rise to the diversity of metallo-macrocycles. In general, heteronuclear metal arrangement within one molecule requires different metal binding sites each of which has an affinity for a specific metal ion. Only a few examples of heteronuclear metal arrangement using a ligand with chemically equivalent metal binding sites are known so far.[7]

Herein, we report a flat macrocyclic ligand **1** which is capable of accommodating two different metal ions by two chemically equivalent metal chelating sites. The macrocycle **1** possesses two centrally directed phenanthroline coordination sites and reacts with Zn(II) or Cu(I) ions to form a homodinuclear Zn(II)-macrocycle or Cu(I)-macrocycle, respectively. Interestingly, when the macrocycle **1** reacts with an equimolar mixture of Cu(I) and Zn(II) ions, a heterodinuclear Cu(I)−Zn(II)-macrocycle is selectively formed in high yield (>90%). Similarly, a heterodinuclear Ag(I)−Zn(II)-macrocycle is obtained from a mixture of Ag(I) and Zn(II) ions (Figure 1). Thus, the spatially restricted cavity of macrocycle **1** provides a platform for heterodinuclear metal arrangement based largely on the metal-centered coordination geometry, charge number, and ligands other than macrocycle **1**.

RESULTS AND DISCUSSION

Design and Synthesis of a Macrocyclic Ligand. A macrocyclic ligand **1** which possesses two phenanthroline coordination sites was synthesized as a platform for metal arrangement. Two coordination sites are directed inward so that two metal ions can be included in a face-to-face fashion within the macrocyclic cavity. The macrocycle **1** was prepared by sequential connections of 2,9-dichloro-1,10-phenanthroline (**6**), 1,4-bis(4,4,5,5-tetramethyl-1,3,2-dioxaborolan-2-yl)-benzene (**7**), and 1,3-dibromo-5-(hexyloxy)benzene (**8**) to

Received: August 18, 2011
Published: January 10, 2012

   dx.doi.org/10.1021/ic201803c | Inorg. Chem. 2012, 51, 1508−1515

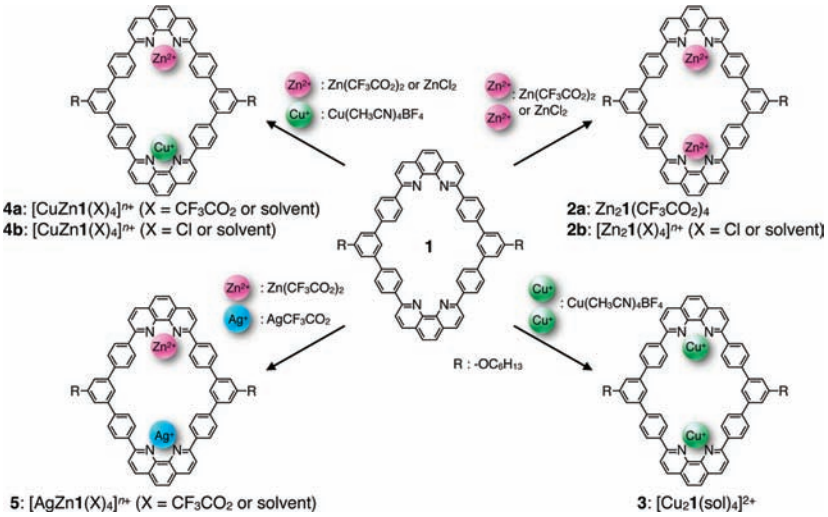

Figure 1. Various metal including macrocycles formed from a macrocyclic ligand **1**.

Scheme 1. Synthesis of Macrocycle 1[a]

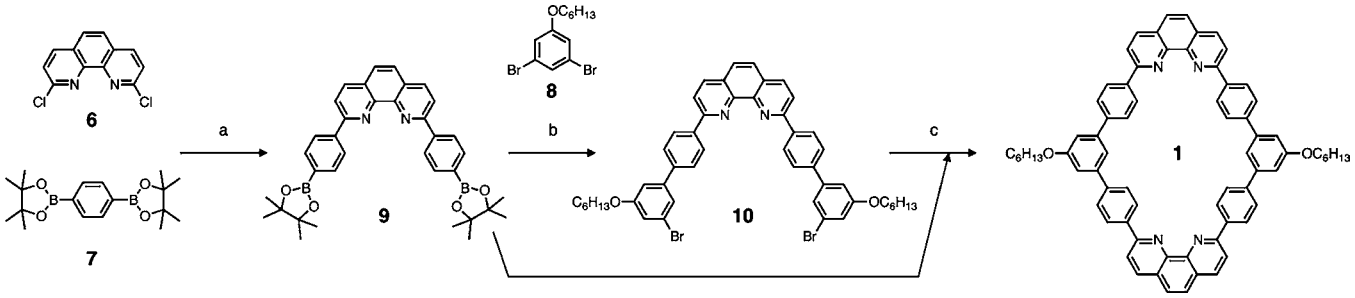

[a]Reagents and conditions: (a) $Pd(PPh_3)_4$, Na_2CO_3, dioxane, ethanol, H_2O, 60 °C, 29%; (b) $Pd(PPh_3)_4$, *n*-Bu_4NBr, Na_2CO_3, toluene, H_2O, 100 °C, 57%; (c) $Pd(PPh_3)_4$, *n*-Bu_4NBr, Na_2CO_3, toluene, H_2O, 90 °C, 15%.

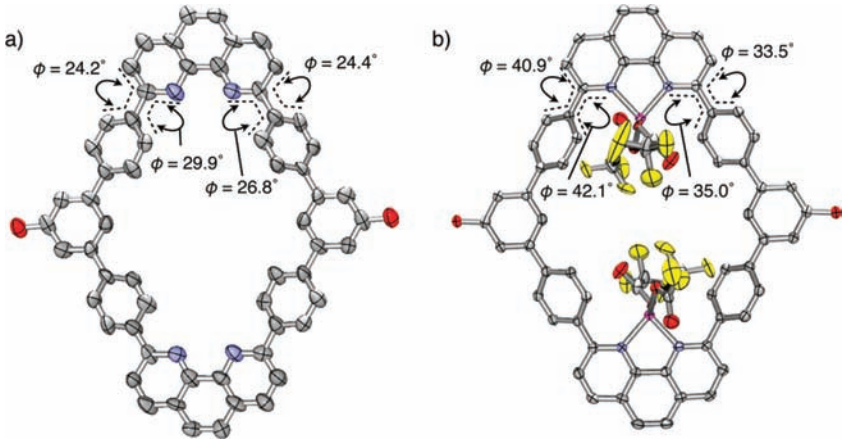

Figure 2. Crystal structures of (a) macrocycle **1** and (b) homodinuclear Zn(II)-macrocycle, Zn_2**1**$(CF_3CO_2)_4$ (**2a**) (solvents, side-alkyl-chains, and hydrogen atoms are omitted for clarity). The molecular structures are represented with 50% thermal ellipsoids. ϕ denotes the dihedral angle.

afford precursors **9** and **10**, followed by the intermolecular cyclization between them by Suzuki–Miyaura coupling (Scheme 1 and Supporting Information, Scheme S1; for the synthetic details, see Supporting Information). The yield of the final cyclization step was 15%. Its rhombic macrocyclic structure with a nanometer-sized cavity (long axis: 1.3 nm, short axis: 0.8 nm) was determined by the X-ray crystal analysis (Figure 2a and Supporting Information, Figure S8). The structure was relatively flat with small dihedral angles between phenanthroline and adjacent benzene rings (C–C–C–C and N–C–C–C; ϕ = 24.2–29.9°).

Homodinuclear Metal Complexes of Macrocycle 1. Macrocycle **1** has two chemically equivalent metal coordination sites capable of binding two identical metal ions within the cavity. First, complexation of **1** with $Zn(CF_3CO_2)_2$ (2.0 equiv) in $CDCl_3/CD_3CN$ = 10:1 resulted in the formation of a homodinuclear Zn(II)-macrocycle, Zn_2**1**$(CF_3CO_2)_4$ (**2a**). In the ^1H NMR spectroscopic titration study, the spectra first

dx.doi.org/10.1021/ic201803c | Inorg. Chem. 2012, 51, 1508–1515

expressed signal patterns corresponding to a complex with C_{2v}-symmetry and then changed to that with D_{2h}-symmetry, suggesting the conversion from a mononuclear intermediate to a dinuclear $Zn_2\mathbf{1}(CF_3CO_2)_4$ with increasing the concentration of Zn(II) ions (Figure 3b and Supporting Information, Figure S9). The phenanthroline proton signals showed downfield shift (signals (a) and (b); $\Delta\delta$ = +0.31 and +0.40 ppm, respectively) because of the Zn(II) binding. Concurrently with the metal binding, *para*-phenylene protons (d) next to the phenanthroline groups showed significant upfield shift ($\Delta\delta$ = −0.70 ppm). This indicates that the shielding effect of phenanthroline groups is induced because of the solution-phase conformational changes of these *para*-phenylene moieties to rotate in a direction perpendicular to the macrocyclic plane. The formation of dinuclear complex, $Zn_2\mathbf{1}(CF_3CO_2)_4$ (**2a**), was also supported by electrospray ionization-time-of-flight (ESI-TOF) mass spectrometry (m/z 1617.4 as $[Zn_2\mathbf{1}(CF_3CO_2)_4 + Na]^+$, Supporting Information, Figure S16).

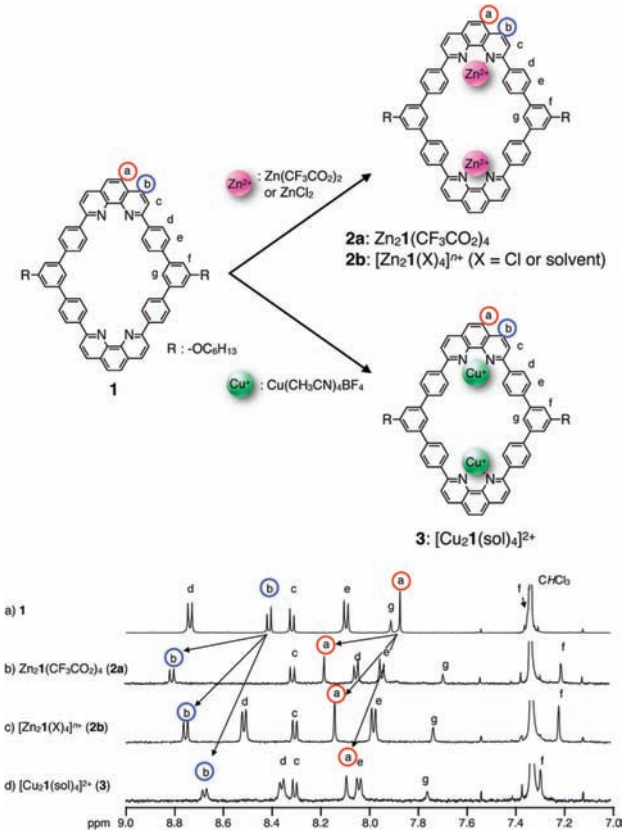

Figure 3. Partial ^{1}H NMR spectra (500 MHz, $CDCl_3/CD_3CN$ = 10:1, 293 K) of (a) macrocycle **1** ([**1**] = 0.30 mM), (b) **2a** ([**1**] = 0.13 mM, $[Zn(CF_3CO_2)_2]$ = 0.26 mM), (c) **2b** ([**1**] = 0.21 mM, $[ZnCl_2]$ = 0.43 mM), (d) **3** ([**1**] = 0.13 mM, $[Cu(CH_3CN)_4BF_4]$ = 0.29 mM).

Furthermore, the crystal structure of $Zn_2\mathbf{1}(CF_3CO_2)_4$ was determined by an X-ray analysis (Figure 2b, Supporting Information, Figures S17, and S18). In the resulting structure, two Zn(II) ions are bound by two phenanthroline sites in the rhombic cavity of **1** with a Zn−Zn distance of 9.43 Å. In addition, two $CF_3CO_2^-$ ions are bound to each Zn(II) ion to result in a tetrahedral coordination geometry with Zn−O bond distances from 1.88 to 1.97 Å. Relatively large dihedral angles between phenanthroline and adjacent benzene (C−C−C−C and N−C−C−C) compared to the metal-free ligand **1** also suggest the steric repulsion between *para*-phenylene rings and $CF_3CO_2^-$ ligands (Figure 2, ϕ = 33.5−42.1° for $Zn_2\mathbf{1}(CF_3CO_2)_4$ whereas ϕ = 24.2−29.9° for **1**). This result is consistent with the upfield shift of proton signals (d) in the ^{1}H NMR spectrum of **2a** in solution.

When $ZnCl_2$ was used instead of $Zn(CF_3CO_2)_2$, another dinuclear Zn(II)-macrocycle was obtained. Upon the addition of $ZnCl_2$ (2.0 equiv) to macrocycle **1** in a $CDCl_3/CD_3CN$ = 10:1 solution, a dinuclear $[Zn_2\mathbf{1}(X)_4]^{n+}$ (**2b**) (X = Cl or solvent) was formed via a mononuclear $[Zn\mathbf{1}(X)_2]^{n+}$ (Figure 3c and Supporting Information, Figure S19, see signals (a) and (b); $\Delta\delta$ = +0.27 and +0.34 ppm, respectively). The ^{1}H NMR spectrum of **2b** also indicated the D_{2h}-symmetrical structure, but it was different from that of **2a** which was formed from **1** and $Zn(CF_3CO_2)_2$ as seen in the proton signals (d) of the *para*-phenylene ring next to phenanthroline ($\Delta\delta$ = −0.70 ppm and −0.23 ppm for **2a** and **2b**, respectively). This result suggests that the two $CF_3CO_2^-$ or Cl^- (or solvent) ligands are bound to each Zn(II) ion to form a tetrahedral coordination geometry and interact differently with the *para*-phenylene rings within the macrocycle. The formation of **2b** was also supported by ESI-TOF mass spectrometry (m/z 607.1 as $[Zn_2\mathbf{1}Cl_2]^{2+}$, Supporting Information, Figure S23).

Furthermore, Cu(I) ions, which prefer a tetrahedral coordination, were also included within the macrocycle. Upon the addition of $Cu(CH_3CN)_4BF_4$ (2.3 equiv) to macrocycle **1** in a $CDCl_3/CD_3CN$ = 10:1 solution, the ^{1}H NMR signals of phenanthroline protons gradually shifted to the lower magnetic field, indicating the complexation between Cu(I) ions and the phenanthroline sites (Figure 3d and Supporting Information, Figure S24, see signals (a) and (b); $\Delta\delta$ = +0.22 and +0.26 ppm, respectively). Different from the case with Zn(II), proton signals for mononuclear $[Cu\mathbf{1}(sol)_2]^+$ and dinuclear $[Cu_2\mathbf{1}(sol)_4]^{2+}$ were not separately observed because the ligand exchange rate was faster than the NMR time scale. The formation of homodinuclear complex $[Cu_2\mathbf{1}(sol)_4]^{2+}$ (**3**) was confirmed by ESI-TOF mass spectrometry measurement (m/z 1268.4 as $[Cu_2\mathbf{1}BF_4(CH_3CN)]^+$, Supporting Information, Figure S26). Complexation of **1** with an alternative Zn(II) source, $Zn(CF_3SO_3)_2$, and other metals favoring a tetrahedral coordination geometry such as $AgCF_3CO_2$ and $Hg(CF_3SO_3)_2$ was further examined but resulted in broadening of ^{1}H NMR signals or forming unidentified precipitates. Thus, the stabilities of discrete homodinuclear metal complexes with **1** significantly depend on the kinds of metal ions and counterions. This also suggests that some counteranions tend to bind to Zn(II) centers under the present condition.

Heterodinuclear Metal Complexes of Macrocycle 1. Heterodinuclear metal arrangement was achieved with macrocycle **1** bearing chemically equivalent metal binding sites. Metal complexation of macrocycle **1** was then examined with two different metal ions, Cu(I)/Zn(II) or Ag(I)/Zn(II). Upon mixing an equimolar mixture of three components, macrocyclic ligand **1**, $Cu(CH_3CN)_4BF_4$, and $Zn(CF_3CO_2)_2$, in a $CDCl_3/CD_3CN$ = 10:1 solution, a new set of signals appeared in the ^{1}H NMR spectrum (Figure 4b) suggesting the formation of a heterodinuclear complex with a C_{2v}-symmetry. The ^{1}H−^{1}H correlation spectroscopy (COSY) and rotating frame Overhauser effect spectroscopy (ROESY) demonstrated that these signals can be assigned to two sets of phenanthroline (protons (a)−(c) and (a′)−(c′)), two sets of *para*-phenylene rings next to phenanthroline (protons (d), (e), (d′), and (e′)), two sets of

dx.doi.org/10.1021/ic201803c | *Inorg. Chem.* 2012, 51, 1508−1515

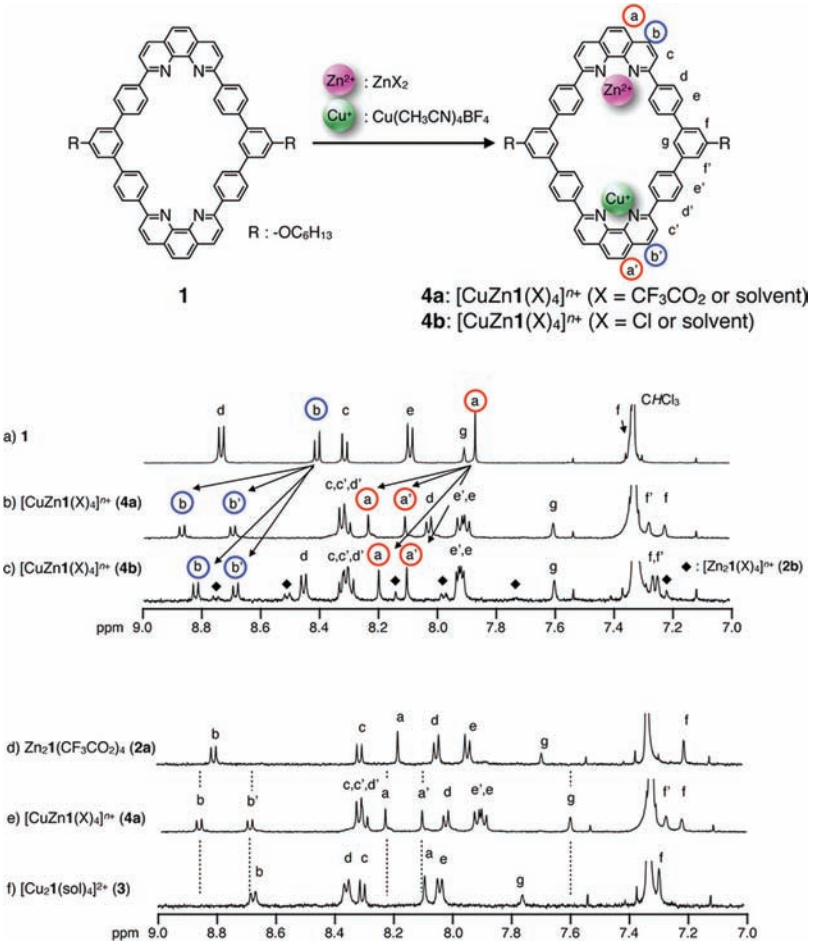

Figure 4. Partial ^{1}H NMR spectra (500 MHz, $CDCl_3/CD_3CN$ = 10:1, 293 K) of (a) macrocycle **1** ([**1**] = 0.30 mM), (b) **4a** ([**1**] = $[Cu(CH_3CN)_4BF_4]$ = $[Zn(CF_3CO_2)_2]$ = 0.24 mM), and (c) **4b** ([**1**] = $[Cu(CH_3CN)_4BF_4]$ = $[ZnCl_2]$ = 0.22 mM). (d–f): Comparison of ^{1}H NMR spectra among homodinuclear Zn(II) (**2a**) and Cu(I) (**3**) complexes and heterodinuclear Cu(I)–Zn(II) complex (**4a**); (d) **2a** ([**1**] = 0.13 mM, $[Zn(CF_3CO_2)_2]$ = 0.26 mM), (e) **4a** ([**1**] = $[Cu(CH_3CN)_4BF_4]$ = $[Zn(CF_3CO_2)_2]$ = 0.24 mM), and (f) **3** ([**1**] = 0.13 mM, $[Cu(CH_3CN)_4BF_4]$ = 0.29 mM).

protons at the *ortho* positions of the side chains (protons (f) and (f′)), and one set of protons at the *para* positions of the side chains (protons (g)) (Supporting Information, Figures S28 and S29). This spectrum was different from those of homodinuclear complexes, $Zn_2\mathbf{1}(CF_3CO_2)_4$ (**2a**) and $[Cu_2\mathbf{1}(sol)_4]^{2+}$ (**3**) (Figures 4d and f). This suggests that the macrocycle **1** includes both Cu(I) and Zn(II) ions to form a heterodinuclear $[CuZn\mathbf{1}(X)_4]^{n+}$ (**4a**) (X = CF_3CO_2 or solvent). Two sets of phenanthrolines and adjacent proton signals ((a)–(f) or (a′)–(f′)) were assigned by comparison of the magnitude of signal shifts with the spectra of homodinuclear complexes **2a** and **3**, for instance, $\Delta\delta$ = +0.36 ppm for signal (a) and $\Delta\delta$ = +0.24 ppm for signal (a′) ($\Delta\delta$: signal shift change relative to signals of free ligand **1**). Thus, signals (a)–(f) and (a′)–(f′) were assigned for protons around Zn(II)-phenanthroline and Cu(I)-phenanthroline, respectively. ESI-TOF mass spectrometry measurement strongly supported the formation of the heterodinuclear complex (m/z 1408.1 as $[CuZn\mathbf{1}(CF_3CO_2)_2(CH_3CN)]^+$, Supporting Information, Figure S30). Unfortunately, no crystals were obtained for X-ray analysis despite attempts under various conditions.

The formation efficiency of the heterodinuclear complex $[CuZn\mathbf{1}(X)_4]^{n+}$ (**4a**) (X = CF_3CO_2 or solvent) from macrocycle **1** in the presence of an equimolar mixture of $Cu(CH_3CN)_4BF_4$ and $Zn(CF_3CO_2)_2$ was estimated to be over 90% from the NMR spectroscopic data. In this reaction, complex **4a** is a thermodynamically controlled product because the same product was obtained regardless of the order of metal addition. To describe this highly selective heterodinuclear complexation in detail, stepwise stability constants of complexation at 20 °C were estimated by UV–vis titration and NMR spectroscopic competition experiments. First, the stability constants K_1^{Zn} and K_2^{Zn} for homogeneous Zn(II)-complex formation (K_1^{Zn} = $[Zn\mathbf{1}(CF_3CO_2)_2]/[\mathbf{1}][Zn(CF_3CO_2)_2]$ M^{-1}, K_2^{Zn} = $[Zn_2\mathbf{1}(CF_3CO_2)_4]/[Zn\mathbf{1}(CF_3CO_2)_2][Zn(CF_3CO_2)_2]$ M^{-1}, respectively, Scheme 2) were calculated using curve fitting on UV–vis titration to be $K_1^{Zn} \geq 10^7$ M^{-1} and K_2^{Zn} = $(1.0 \pm 0.4) \times 10^6$ M^{-1} (Supporting Information, Figure S31). Similarly, the stability constants K_1^{Cu} and K_2^{Cu} for homogeneous Cu(I)-complex formation (K_1^{Cu} = $[[Cu\mathbf{1}(sol)_2]^+]/[\mathbf{1}][[Cu(CH_3CN)_4]^+]$ M^{-1}, K_2^{Cu} = $[[Cu_2\mathbf{1}(sol)_4]^{2+}]/[[Cu\mathbf{1}(sol)_2]^+][[Cu(CH_3CN)_4]^+]$ M^{-1}, respectively, Scheme 2) were estimated to be $K_1^{Cu} = (4 \pm 3) \times 10^6$ M^{-1} and K_2^{Cu} = $(1.1 \pm 0.2) \times 10^5$ M^{-1} (Supporting Information, Figure S33). Next, the stability constants K_2^{ZnCu} and K_2^{CuZn} for heterodinuclear Cu(I)–Zn(II)-complex formation (K_2^{ZnCu} = $[[CuZn\mathbf{1}(X)_4]^{n+}]/[Zn\mathbf{1}(CF_3CO_2)_2][[Cu(CH_3CN)_4]^+]$ M^{-1}, K_2^{CuZn} = $[[CuZn\mathbf{1}(X)_4]^{n+}]/[[Cu\mathbf{1}(sol)_2]^+][Zn(CF_3CO_2)_2]$

dx.doi.org/10.1021/ic201803c | *Inorg. Chem.* 2012, 51, 1508–1515

Scheme 2. Equilibrium Diagram for the Formation of Homo- and Heterodinuclear Metal Complexes

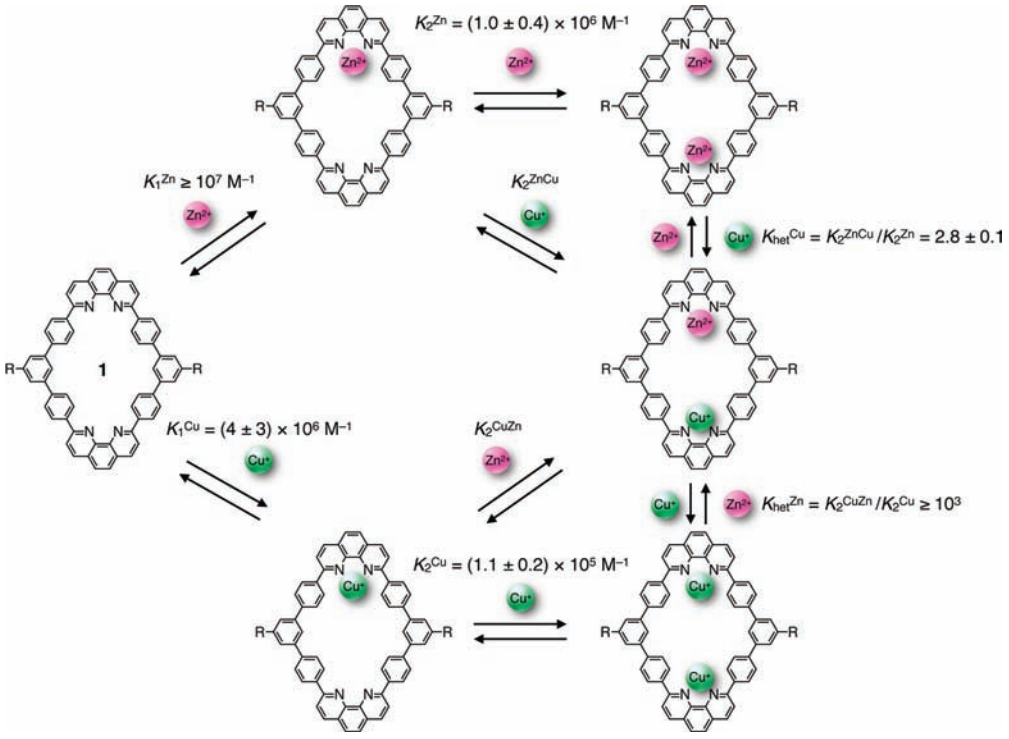

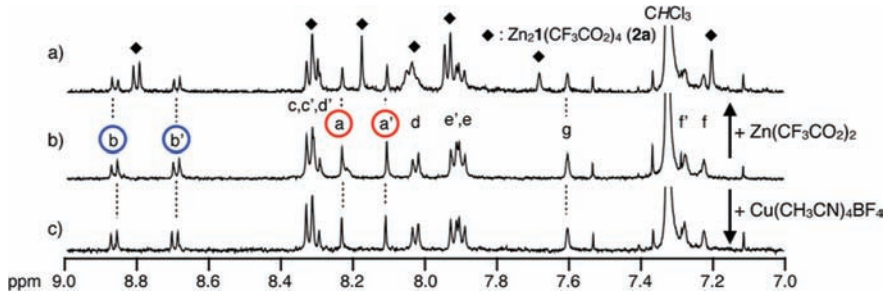

Figure 5. Partial ^{1}H NMR spectra of **1** at different mixing ratios of $Cu(CH_3CN)_4BF_4$ and $Zn(CF_3CO_2)_2$ (500 MHz, $CDCl_3/CD_3CN$ = 10:1, 293 K): (a) [**1**] = 0.18 mM, $[Cu(CH_3CN)_4BF_4]$ = 0.18 mM (1.0 equiv), $[Zn(CF_3CO_2)_2]$ = 0.54 mM (3.0 equiv), (b) [**1**] = 0.28 mM, $[Cu(CH_3CN)_4BF_4]$ = 0.28 mM (1.0 equiv), $[Zn(CF_3CO_2)_2]$ = 0.28 mM (1.0 equiv), and (c) [**1**] = 0.11 mM, $[Cu(CH_3CN)_4BF_4]$ = 0.99 mM (9.0 equiv), $[Zn(CF_3CO_2)_2]$ = 0.11 mM (1.0 equiv).

M^{-1}, respectively, Scheme 2) were evaluated by NMR spectroscopic competition experiments (Figure 5). When 1.0 equiv of $Cu(CH_3CN)_4BF_4$ and 3.0 equiv of $Zn(CF_3CO_2)_2$ were added to **1** ([**1**] = 0.18 mM), $[CuZn\mathbf{1}(X)_4]^{n+}$ and $Zn_2\mathbf{1}(CF_3CO_2)_4$ were formed in about 1:1 ratio (Figure 5a), which reveal the stability constant ratio K_2^{ZnCu}/K_2^{Zn} to be about 2.8. On the other hand, when 9.0 equiv of $Cu(CH_3CN)_4BF_4$ and 1.0 equiv of $Zn(CF_3CO_2)_2$ were added to **1** ([**1**] = 0.11 mM), $[CuZn\mathbf{1}(X)_4]^{n+}$ was quantitatively formed (Figure 5c), which indicates that the stability constant ratio is $K_2^{CuZn}/K_2^{Cu} \geq 10^3$. Here, $K_2^{ZnCu}/K_2^{Zn} = [[CuZn\mathbf{1}(X)_4]^{n+}][Zn(CF_3CO_2)_2]/[Zn_2\mathbf{1}(CF_3CO_2)_4][[Cu(CH_3CN)_4]^+]$ means the equilibrium constant between $[CuZn\mathbf{1}(X)_4]^{n+}$ and $Zn_2\mathbf{1}(CF_3CO_2)_4$, hereafter referred to as K_{het}^{Cu}. Similarly, $K_2^{CuZn}/K_2^{Cu} = [[CuZn\mathbf{1}(X)_4]^{n+}][[Cu(CH_3CN)_4]^+]/[[Cu\mathbf{1}(sol)_4]^{2+}][Zn(CF_3CO_2)_2]$ is referred to as K_{het}^{Zn} (Scheme 2). Using these stability constants, that of the heterodinuclear complexation (eq [1]), $K = [[CuZn\mathbf{1}(X)_4]^{n+}]^2/[Zn_2\mathbf{1}(CF_3CO_2)_4][[Cu_2\mathbf{1}(sol)_4]^{2+}]$, was calculated as $K_{het}^{Cu} \times K_{het}^{Zn}$ to be $\geq 10^3$, indicating that the ratio of $[CuZn\mathbf{1}(X)_4]^{n+}$ is much greater than 94% under the given condition.

$$Zn_2\mathbf{1}(CF_3CO_2)_4 + [Cu_2\mathbf{1}(sol)_4]^{2+} \rightleftarrows 2[CuZn\mathbf{1}(X)_4]^{n+} \quad (1)$$

The selective formation of the heterodinuclear Cu(I)−Zn(II)-complex from an equimolar mixture of $Cu(CH_3CN)_4BF_4$ and $Zn(CF_3CO_2)_2$ with **1** can be well explained by this high constant value. In other words, this selectivity arises from the high value of K_{het}^{Zn} because of the low stability of the homodinuclear Cu(I)-complex. The ionic characteristic of $[Cu_2\mathbf{1}(sol)_4](BF_4)_2$ may cause the relative destabilization in the solvation process.

For the compositional formula of the heterodinuclear complex, $[CuZn\mathbf{1}(CF_3CO_2)_2(CH_3CN)_2]^+$ is the most likely structure based on the mass spectrometry data, that is, two CH_3CN molecules and two $CF_3CO_2^-$ ions are presumed to bind to Cu(I) and Zn(II) ions, respectively. The effects of counterions on the formation of heterodinuclear Cu(I)−Zn(II)-macrocycle was then examined by changing the metal

dx.doi.org/10.1021/ic201803c | Inorg. Chem. 2012, 51, 1508−1515

sources. First, 1 equiv of $Cu(CH_3CN)_4BF_4$ and 1 equiv of $ZnCl_2$ instead of $Zn(CF_3CO_2)_2$ were mixed with macrocycle **1** in a $CDCl_3/CD_3CN$ = 10:1 solution. The ^1H NMR spectrum of the resulting solution involved one set of signals similar to that of **4a** with $Zn(CF_3CO_2)_2$, suggesting the formation of $[CuZn\mathbf{1}(X)_4]^{n+}$ (**4b**) (X = Cl or solvent) in 59% yield, whereas the formation efficiency was not so high as the case with **4a** (Figure 4c). ESI-TOF mass spectrometry measurement demonstrated the heterodinuclear metal arrangement (m/z 1252.3 as $[CuZn\mathbf{1}Cl_2(CH_3CN)]^+$, Supporting Information, Figure S37). In contrast, when $Zn(CF_3SO_3)_2$ was used instead, no heterodinuclear Cu(I)−Zn(II)-macrocycle was observed in ^1H NMR spectrum but the observed signals were broadened, suggesting the formation of some aggregates.[8] Thus, the kind of counterions has a strong influence on the metal arrangement especially when two different metals coexist.

Furthermore, not only Cu(I) but also Ag(I) ions (3 equiv of $AgCF_3CO_2$) capable of adopting a tetrahedral coordination geometry provided another heterodinuclear Ag(I)−Zn(II)-macrocycle $[AgZn\mathbf{1}(X)_4]^{n+}$ (**5**) (X = CF_3CO_2 or solvent) in the presence of macrocycle **1** and 2 equiv of $Zn(CF_3CO_2)_2$ in a $CDCl_3/CD_3CN$ = 10:1 solution. The ^1H NMR spectrum of the resulting solution indicated the formation of **5** with C_{2v}-symmetry in 60% yield (Supporting Information, Figure S38). ESI-TOF mass spectrometry measurement demonstrated the formation of **5** (m/z 1411.6 as $[AgZn\mathbf{1}(CF_3CO_2)_2]^+$, Supporting Information, Figure S41).

In summary, three different heterodinuclear metallo-macrocycles, $[CuZn\mathbf{1}(X)_4]^{n+}$ (**4a**) (X = CF_3CO_2 or solvent), $[CuZn\mathbf{1}(X)_4]^{n+}$ (**4b**) (X = Cl or solvent), and $[AgZn\mathbf{1}(X)_4]^{n+}$ (**5**) (X = CF_3CO_2 or solvent), were obtained with high selectivity. It should be noted that other combinations of M-Zn(II) (M = Li(I), Mg(II), Pd(II), Hg(II), La(III), or Tb(III)) resulted in the formation of unidentifiable mixtures or aggregates.

CONCLUSION

We have designed and synthesized macrocycle **1** with two chemically equivalent phenanthroline sites for homo- or heterodinuclear metal arrangement. It was deduced from the molecular structure of homodinuclear $Zn_2\mathbf{1}(CF_3CO_2)_4$ that the most stable coordination geometry of two metal centers is tetrahedral in common in the spatially restricted macrocyclic cavity. Metal ions such as Cu(I) and Ag(I) which prefer a tetrahedral coordination geometry also formed heterodinuclear Cu(I)−Zn(II)- and Ag(I)−Zn(II)-macrocycles with high selectivity. Overall, heterodinuclear metal arrangement within the spatially restricted cavity of macrocycle **1** depends on the metal-centered coordination geometry, charge number, and ligands (counterions and solvent molecules) bound to the metal centers. Such heteronuclear metal arrangement within a molecule possessing multiple, chemically equivalent metal binding sites would provide a clue to metal-based multipoint molecular recognition for catalysis.

EXPERIMENTAL SECTION

Materials and General Methods. All solvents, organic and inorganic reagents are commercially available, and were used without further purification. $Pd(PPh_3)_4$,[9] $Zn(CF_3CO_2)_2$,[10] and $Zn(CF_3CO_2)_2(DME)$[10] were synthesized according to previously reported procedures. The purity of $Zn(CF_3CO_2)_2$ was determined by ethylenediaminetetraacetate (EDTA) titration using Xylenol Orange as an indicator. Silica gel column chromatography was performed using Merck Silica Gel 60 (230−400 mesh). NMR spectroscopic measurements were performed using a Bruker DRX 500 spectrometer. NMR spectra are calibrated as below; $CDCl_3$ only or $CDCl_3/CD_3CN$ = 10:1: tetramethylsilane ($Si(CH_3)_4$) = 0 ppm for ^1H, $CDCl_3$ = 77.16 ppm for ^{13}C; DMSO-d_6: $(CHD_2)(CD_3)SO$ = 2.50 ppm for ^1H; CD_3OD: CHD_2OD = 3.31 ppm for ^1H, CD_3OD = 49.00 ppm for ^{13}C. Electrospray ionization-time-of-flight (ESI-TOF) mass spectra were recorded on a Micromass LCT spectrometer. UV−vis spectroscopy was performed using a HITACHI U-3500 spectrophotometer. IR spectra were obtained with a JASCO FT/IR 4200 spectrometer using a ZnSe ATR method. Melting point was measured using a Yanaco MP-500D apparatus. Gel permeation chromatography (GPC) was performed on a recycling preparative HPLC (Japan Analytical Industry; LC-928) with a JAIGEL-2H-40 column. Single-crystal X-ray crystallographic analyses were performed using a Rigaku RAXIS-RAPID imaging plate diffractometer with MoKα radiation, and obtained data were calculated using the CrystalStructure crystallographic software package except for refinement, which was performed using SHELXL-97.[11] X-ray structures were displayed using Mercury and ORTEP-3 programs. The synthetic procedure of **1** is described in the Supporting Information.

Preparation of $Zn_2\mathbf{1}(CF_3CO_2)_4$ (2a). To a solution of **1** in $CDCl_3/CD_3CN$ = 10:1 (150 μM, 600 μL, 0.090 μmol, 1.0 equiv) was added a solution of $Zn(CF_3CO_2)_2$ in CD_3CN (16.5 mM, 11 μL, 0.18 μmol, 2.0 equiv). $CDCl_3$ was added to keep the solvent ratio ($CDCl_3/CD_3CN$ = 10:1) constant. *p*-Dimethoxybenzene (100 μM) was used as an internal standard. The single crystal for X-ray analysis was obtained by slow evaporation of a solution of **1** (141 μM) and $Zn(CF_3CO_2)_2(DME)$ (50 equiv) in $CDCl_3/CD_3CN$ = 10:1.

^1H NMR (500 MHz, $CDCl_3/CD_3CN$ = 10:1, 293 K): δ 8.81 (d, J = 8.4 Hz, 4H, Ar*H*), 8.31 (d, J = 8.4 Hz, 4H, Ar*H*), 8.18 (s, 4H, Ar*H*), 8.04 (d, J = 7.8 Hz, 8H, Ar*H*), 7.94 (d, J = 7.3 Hz, 8H, Ar*H*), 7.68 (s, 2H, Ar*H*), 7.20 (s, 4H, Ar*H*), 4.15 (t, J = 6.5 Hz, 4H, CH_2), 1.90−1.80 (m, 4H, CH_2, behind the H_2O peak), 1.57−1.53 (m, 4H, CH_2), 1.42−1.38 (m, 8H, CH_2), 0.94 (t, J = 7.0 Hz, 6H, CH_3).

^{13}C NMR (125 MHz, $CDCl_3/CD_3CN$ = 10:1, 293 K): δ 159.4 (C_q), 144.1 (C_q), 142.4 (C_q), 141.1 (*C*H), 141.0 (C_q), 136.5 (C_q), 136.2 (C_q), 129.0 (*C*H), 128.4 (C_q), 128.4 (*C*H), 128.4 (*C*H), 126.9 (*C*H), 125.8 (*C*H), 113.4 (*C*H), 68.3 (CH_2), 31.5 (CH_2), 29.2 (CH_2), 25.7 (CH_2), 22.5 (CH_2), 13.9 (CH_3).

ESI-MS: m/z calcd for $[Zn_2\mathbf{1}(CF_3CO_2)_4 + Na]^+$: 1617.26; found: 1617.35.

Crystal Structure. Detail data and a cif file are in the Supporting Information. CCDC reference number: 785929.

Preparation of $[Zn_2\mathbf{1}(X)_4]^{n+}$ (2b) (X = Cl or solvent). To a solution of **1** in $CDCl_3/CD_3CN$ = 10:1 (270 μM, 300 μL, 0.081 μmol, 1.0 equiv) was added a solution of $ZnCl_2$ in CD_3CN (25 mM, 6.4 μL, 0.16 μmol, 2.0 equiv). $CDCl_3$ was added to keep the solvent ratio ($CDCl_3/CD_3CN$ = 10:1) constant. *p*-Dimethoxybenzene (100 μM) was used as an internal standard.

^1H NMR (500 MHz, $CDCl_3/CD_3CN$ = 10:1, 293 K): δ 8.75 (d, J = 8.3 Hz, 4H, Ar*H*), 8.51 (d, J = 7.5 Hz, 8H, Ar*H*), 8.30 (d, J = 8.3 Hz, 4H, Ar*H*), 8.14 (s, 4H, Ar*H*), 7.98 (d, J = 7.8 Hz, 8H, Ar*H*), 7.73 (s, 2H, Ar*H*), 7.21 (s, 4H, Ar*H*), 4.16 (t, J = 6.5 Hz, 4H, CH_2), 1.90−1.80 (m, 4H, CH_2, partially behind the H_2O peak), 1.58−1.53 (m, 4H, CH_2), 1.43−1.39 (m, 8H, CH_2), 0.95 (t, J = 6.5 Hz, 6H, CH_3).

ESI-MS: m/z calcd for $[Zn_2\mathbf{1}Cl_2]^{2+}$: 607.13; found: 607.09. Although the formation ratio in solution remains unknown, tetranuclear species $[Zn_4\mathbf{1}Cl_6]^{2+}$ (calcd: 743.00; found: 742.95) and $[Zn_4\mathbf{1}Cl_7]^+$ (calcd: 1522.96; found: 1522.88) were also observed.

Preparation of $[Cu_2\mathbf{1}(sol)_4]^{2+}$ (3). To a solution of **1** in $CDCl_3/CD_3CN$ = 10:1 (150 μM, 630 μL, 0.095 μmol, 1.0 equiv) was added a solution of $Cu(CH_3CN)_4BF_4$ in CD_3CN (20 mM, 10.6 μL, 0.21 μmol, 2.3 equiv). $CDCl_3$ was added to keep the solvent ratio ($CDCl_3/CD_3CN$ = 10:1) constant. *p*-Dimethoxybenzene (100 μM) was used as an internal standard.

^1H NMR (500 MHz, $CDCl_3/CD_3CN$ = 10:1, 293 K): δ 8.67 (d, J = 8.3 Hz, 4H, Ar*H*), 8.35 (d, J = 8.0 Hz, 8H, Ar*H*), 8.30 (d, J = 8.3 Hz, 4H, Ar*H*), 8.09 (s, 4H, Ar*H*), 8.04 (d, J = 7.9 Hz, 8H, Ar*H*), 7.76 (s, 2H, Ar*H*), 7.29 (s, 4H, Ar*H*), 4.19 (t, J = 6.4 Hz, 4H, CH_2), 1.90−1.80

dx.doi.org/10.1021/ic201803c | *Inorg. Chem.* 2012, 51, 1508−1515

(m, 4H, CH_2, partially behind the H_2O peak), 1.61−1.54 (m, 4H, CH_2), 1.46−1.38 (m, 8H, CH_2), 0.96 (t, J = 6.8 Hz, 6H, CH_3).

ESI-MS: m/z calcd for $[Cu_2\mathbf{1}BF_4(CH_3CN)]^+$: 1268.36; found: 1268.44.

Preparation of $[CuZn\mathbf{1}(X)_4]^{n+}$ (4a) (X = CF_3CO_2 or solvent). To a solution of **1** in $CDCl_3/CD_3CN$ = 10:1 (300 μM, 300 μL, 0.090 μmol, 1.0 equiv) was added a solution of $Cu(CH_3CN)_4BF_4$ in CD_3CN (26 mM, 3.4 μL, 0.090 μmol, 1.0 equiv) and a solution of $Zn(CF_3CO_2)_2$ in CD_3CN (26 mM, 3.4 μL, 0.090 μmol, 1.0 equiv). $CDCl_3$ was added to keep the solvent ratio ($CDCl_3/CD_3CN$ = 10:1) constant. *p*-Dimethoxybenzene (100 μM) was used as an internal standard.

^1H NMR (500 MHz, $CDCl_3/CD_3CN$ = 10:1, 293 K): δ 8.87 (d, J = 8.3 Hz, 2H, Ar*H*), 8.70 (d, J = 8.3 Hz, 2H, Ar*H*), 8.33−8.30 (m, 8H, Ar*H*), 8.23 (s, 2H, Ar*H*), 8.11 (s, 2H, Ar*H*), 8.03 (d, J = 7.9 Hz, 4H, Ar*H*), 7.93−7.89 (m, 8H, Ar*H*), 7.60 (s, 2H, Ar*H*), 7.28 (s, 2H, Ar*H*), 7.22 (s, 2H, Ar*H*), 4.17 (t, J = 6.6 Hz, 4H, CH_2), 1.90−1.80 (m, 4H, CH_2, partially behind the H_2O peak), 1.58−1.54 (m, 4H, CH_2), 1.43−1.39 (m, 8H, CH_2), 0.95 (t, J = 6.8 Hz, 6H, CH_3).

ESI-MS: m/z calcd for $[CuZn\mathbf{1}(CF_3CO_2)_2(CH_3CN)]^+$: 1408.33; found: 1408.05.

Preparation of $[CuZn\mathbf{1}(X)_4]^{n+}$ (4b) (X = Cl or solvent). To a solution of **1** in $CDCl_3/CD_3CN$ = 10:1 (240 μM, 340 μL, 0.081 μmol, 1.0 equiv) was added a solution of $Cu(CH_3CN)_4BF_4$ in CD_3CN (20 mM, 4.0 μL, 0.080 μmol, 1.0 equiv) and a solution of $ZnCl_2$ in CD_3CN (23 mM, 3.5 μL, 0.081 μmol, 1.0 equiv). $CDCl_3$ was added to keep the solvent ratio ($CDCl_3/CD_3CN$ = 10:1) constant. *p*-Dimethoxybenzene (100 μM) was used as an internal standard.

^1H NMR (500 MHz, $CDCl_3/CD_3CN$ = 10:1, 293 K): δ 8.82 (d, J = 8.5 Hz, 2H, Ar*H*), 8.69 (d, J = 8.3 Hz, 2H, Ar*H*), 8.45 (d, J = 8.1 Hz, 4H, Ar*H*), 8.33−8.28 (m, 8H, Ar*H*), 8.20 (s, 2H, Ar*H*), 8.10 (s, 2H, Ar*H*), 7.93−7.90 (m, 8H, Ar*H*), 7.60 (s, 2H, Ar*H*), 7.26 (s, 2H, Ar*H*), 7.25 (s, 2H, Ar*H*), 4.18 (t, J = 6.3 Hz, 4H, CH_2), 1.90−1.80 (m, 4H, CH_2, behind the H_2O peak), 1.58−1.54 (m, 4H, CH_2), 1.42−1.39 (m, 8H, CH_2), 0.95 (t, J = 7.0 Hz, 6H, CH_3).

ESI-MS: m/z calcd for $[CuZn\mathbf{1}Cl_2(CH_3CN)]^+$: 1252.29; found: 1252.26.

Preparation of $[AgZn\mathbf{1}(X)_4]^{n+}$ (5) (X = CF_3CO_2 or solvent). To a solution of **1** in $CDCl_3/CD_3CN$ = 10:1 (300 μM, 300 μL, 0.09 μmol, 1.0 equiv) was added a solution of $AgCF_3CO_2$ in CD_3CN (26 mM, 10.2 μL, 0.27 μmol, 3.0 equiv) and a solution of $Zn(CF_3CO_2)_2$ in CD_3CN (26 mM, 6.8 μL, 0.18 μmol, 2.0 equiv). $CDCl_3$ was added to keep the solvent ratio ($CDCl_3/CD_3CN$ = 10:1) constant. *p*-Dimethoxybenzene (100 μM) was used as an internal standard.

^1H NMR (500 MHz, $CDCl_3/CD_3CN$ = 10:1, 293 K): δ 8.87 (d, J = 8.5 Hz, 2H, Ar*H*), 8.69 (d, J = 8.1 Hz, 2H, Ar*H*), 8.32 (d, J = 8.2 Hz, 2H, Ar*H*), 8.29 (d, J = 8.3 Hz, 2H, Ar*H*), 8.25−8.23 (m, 6H, Ar*H*), 8.11 (s, 2H, Ar*H*), 8.02 (d, J = 7.9 Hz, 4H, Ar*H*), 7.95 (d, J = 7.9 Hz, 4H, Ar*H*), 7.86 (d, J = 8.1 Hz, 4H, Ar*H*), 7.41 (s, 2H, Ar*H*), 7.28 (s, 2H, Ar*H*), 7.22 (s, 2H, Ar*H*), 4.17 (t, J = 6.4 Hz, 4H, CH_2), 1.90−1.80 (m, 4H, CH_2, behind the H_2O peak), 1.62−1.54 (m, 4H, CH_2), 1.46−1.39 (m, 8H, CH_2), 0.95 (t, J = 6.6 Hz, 6H, CH_3).

ESI-MS: m/z calcd for $[AgZn\mathbf{1}(CF_3CO_2)_2]^+$: 1411.28; found: 1411.59.

■ ASSOCIATED CONTENT

Ⓢ Supporting Information

Synthetic procedure of **1**, ESI-TOF mass and NMR spectra of **1** and its metal complexes, UV−vis spectra of **2a**, **2b**, and **3**, and X-ray crystallographic data of **1** and **2a** in cif format. This material is available free of charge via the Internet at http://pubs.acs.org.

■ AUTHOR INFORMATION

Corresponding Author

*E-mail: shionoya@chem.s.u-tokyo.ac.jp.

■ ACKNOWLEDGMENTS

This study was supported by Grants-in-Aids from MEXT of Japan and Global COE Program for Chemistry Innovation through Cooperation of Science and Engineering.

■ REFERENCES

(1) (a) Pilkington, N. H.; Robson, R. *Aust. J. Chem.* **1970**, *23*, 2225−2236. (b) Vigato, P. A.; Tamburini, S.; Bertolo, L. *Coord. Chem. Rev.* **2007**, *251*, 1311−1492. (c) Brooker, S. *Eur. J. Inorg. Chem.* **2002**, 2535−2547. (d) Akine, S.; Nabeshima, T. *Dalton Trans.* **2009**, 10395−10408. (e) Tandon, S. S.; Bunge, S. D.; Thompson, L. K. *Chem. Commun.* **2007**, 798−800. (f) McKee, V.; Shepard, W. B. *J. Chem. Soc., Chem. Commun.* **1985**, 158−159. (g) Feltham, H. L. C.; Clérac, R.; Powell, A. K.; Brooker, S. *Inorg. Chem.* **2011**, *50*, 4232−4234. (h) Frischmann, P. D.; Gallant, A. J.; Chong, J. H.; MacLachlan, M. J. *Inorg. Chem.* **2008**, *47*, 101−112. (i) Ma, C. T. L.; MacLachlan, M. J. *Angew. Chem., Int. Ed.* **2005**, *44*, 4178−4182. (j) Akine, S.; Utsuno, F.; Nabeshima, T. *Chem. Commun.* **2010**, *46*, 1029−1031. (k) Huang, W.; Zhu, H.-B.; Gou, S.-H. *Coord. Chem. Rev.* **2006**, *250*, 414−423. (l) van Veggel, F. C. J. M.; Bos, M.; Harkema, S.; Verboom, W.; Reinhoudt, D. N. *Angew. Chem., Int. Ed. Engl.* **1989**, *28*, 746−748. (m) Devoille, A. M. J.; Richardson, P.; Bill, N. L.; Sessler, J. L.; Love, J. B. *Inorg. Chem.* **2011**, *50*, 3116−3126. (n) Chichak, K. S.; Cantrill, S. J.; Pease, A. R.; Chiu, S.-H.; Cave, G. W. V.; Atwood, J. L.; Stoddart, J. F. *Science* **2004**, *304*, 1308−1312. (o) Branscombe, N. D. J.; Blake, A. J.; Marin-Becerra, A.; Li, W.-S.; Parsons, S.; Ruiz-Ramirez, L.; Schröder, M. *Chem. Commun.* **1996**, 2573−2574.

(2) (a) Sessler, J. L.; Tomat, E. *Acc. Chem. Res.* **2007**, *40*, 371−379. (b) Weghorn, S. J.; Sessler, J. L.; Lynch, V.; Baumann, T. F.; Sibert, J. W. *Inorg. Chem.* **1996**, *35*, 1089−1090. (c) Srinivasan, A.; Ishizuka, T.; Osuka, A.; Furuta, H. *J. Am. Chem. Soc.* **2003**, *125*, 878−879. (d) Tanaka, Y.; Saito, S.; Mori, S.; Aratani, N.; Shinokubo, H.; Shibata, N.; Higuchi, Y.; Yoon, Z. S.; Kim, K. S.; Noh, S. B.; Park, J. K.; Kim, D.; Osuka, A. *Angew. Chem., Int. Ed.* **2008**, *47*, 681−684. (e) Gokulnath, S.; Yamaguchi, K.; Toganoh, M.; Mori, S.; Uno, H.; Furuta, H. *Angew. Chem., Int. Ed.* **2011**, *50*, 2302−2306. (f) Charrière, R.; Jenny, T. A.; Rexhausen, H.; Gossauer, A. *Heterocycles* **1993**, *36*, 1561−1575. (g) Narayanan, S. J.; Sridevi, B.; Chandrashekar, T. K.; Englich, U.; Ruhlandt-Senge, K. *Inorg. Chem.* **2001**, *40*, 1637−1645.

(3) (a) Yamaguchi, Y.; Kobayashi, S.; Miyamura, S.; Okamoto, Y.; Wakamiya, T.; Matsubara, Y.; Yoshida, Z. *Angew. Chem., Int. Ed.* **2004**, *43*, 366−369. (b) Bazzicalupi, C.; Bencini, A.; Berni, E.; Bianchi, A.; Fornasari, P.; Giorgi, C.; Valtancoli, B. *Inorg. Chem.* **2004**, *43*, 6255−6265. (c) Dietrich-Buchecker, C. O.; Guilhem, J.; Pascard, C.; Sauvage, J.-P. *Angew. Chem., Int. Ed. Engl.* **1990**, *29*, 1154−1156. (d) Schmittel, M.; Ganz, A.; Fenske, D. *Org. Lett.* **2002**, *4*, 2289−2292.

(4) (a) Amendola, V.; Fabbrizzi, L.; Mangano, C.; Pallavicini, P.; Poggi, A.; Taglietti, A. *Coord. Chem. Rev.* **2001**, *219*−*221*, 821−837. (b) Martell, A. E.; Perutka, J.; Kong, D. *Coord. Chem. Rev.* **2001**, *216*−*217*, 55−63. (c) Lehn, J.-M.; Pine, S. H.; Watanabe, E.; Willard, A. K. *J. Am. Chem. Soc.* **1977**, *99*, 6766−6768. (d) Hao, H.-G.; Zheng, X.-D.; Lu, T.-B. *Angew. Chem., Int. Ed.* **2010**, *49*, 8148−8151. (e) Bazzicalupi, C.; Bencini, A.; Bianchi, A.; Fusi, V.; Giorgi, C.; Paoletti, P.; Valtancoli, B.; Zanchi, D. *Inorg. Chem.* **1997**, *36*, 2784−2790. (f) Li, S.-A.; Li, D.-F.; Yang, D.-X.; Li, Y.-Z.; Huang, J.; Yu, K.-B.; Tang, W.-X. *Chem. Commun.* **2003**, 880−881.

(5) (a) Xu, W.; Rourke, J. P.; Vittal, J. J.; Puddephatt, R. J. *J. Chem. Soc., Chem. Commun.* **1993**, 145−147. (b) Xu, W.; Vittal, J. J.; Puddephatt, R. J. *J. Am. Chem. Soc.* **1995**, *117*, 8362−8371. (c) Zhang, Q.-F.; Adams, R. D.; Fenske, D. *J. Mol. Struct.* **2005**, *741*, 129−134.

(6) (a) Alberts, A. H.; Annunziata, R.; Lehn, J.-M. *J. Am. Chem. Soc.* **1977**, *99*, 8502−8504. (b) Louis, R.; Agnus, Y.; Weiss, R. *J. Am. Chem. Soc.* **1978**, *100*, 3604−3605. (c) Kajiwara, T.; Iki, N.; Yamashita, M. *Coord. Chem. Rev.* **2007**, *251*, 1734−1746. (d) Kajiwara, T.; Kon, N.; Yokozawa, S.; Ito, T.; Iki, N.; Miyano, S. *J. Am. Chem. Soc.* **2002**, *124*, 11274−11275.

(7) (a) Hiraoka, S.; Goda, M.; Shionoya, M. *J. Am. Chem. Soc.* **2009**, *131*, 4592−4593. (b) Gagné, R. R.; Spiro, C. L.; Smith, T. J.; Hamann,

C. A.; Thies, W. R.; Shiemke, A. K. *J. Am. Chem. Soc.* **1981**, *103*, 4073−4081. (c) Dutta, S. K.; Werner, R.; Flörke, U.; Mohanta, S.; Nanda, K. K.; Haase, W.; Nag, K. *Inorg. Chem.* **1996**, *35*, 2292−2300. (d) Lisowski, J. *Inorg. Chim. Acta* **1999**, *285*, 233−240. (e) Lewis, D. J.; Glover, P. B.; Solomons, M. C.; Pikramenou, Z. *J. Am. Chem. Soc.* **2011**, *133*, 1033−1043. (f) Odabaş, Z.; Dumludağ, F.; Özkaya, A. R.; Yamauchi, S.; Kobayashi, N.; Bekaroğlu, Ö. *Dalton Trans.* **2010**, *39*, 8143−8152. (g) Arnold, P. L.; Patel, D.; Wilson, C.; Love, J. B. *Nature* **2008**, *451*, 315−318. (h) Kadish, K. M.; Frémond, L.; Burdet, F.; Barbe, J.-M.; Gros, C. P.; Guilard, R. *J. Inorg. Biochem.* **2006**, *100*, 858−868.

(8) Macrocycle **1** often forms submicrometer-scale aggregates with Zn(II) ions under some conditions as observed by AFM study. In such cases, we observed the broadening of the ^{1}H NMR signals. We will report the details elsewhere.

(9) Coulson, D. R. *Inorg. Synth.* **1972**, *13*, 121−124.

(10) Dell'Amico, D. B.; Boschi, D.; Calderazzo, F.; Labella, L.; Marchetti, F. *Inorg. Chim. Acta* **2002**, *330*, 149−154.

(11) Sheldrick, G. M. *SHELXL-97, Program for refinement of crystal structures*; University of Göttingen: Göttingen, Germany, 1997.